BIOLOGY OF REPRODUCTION (2012) **87**(2):49, 1–11
Published online before print 30 May 2012.
DOI 10.1095/biolreprod.111.097675

Slc2a8 Deficiency in Mice Results in Reproductive and Growth Impairments[1]

Katie L. Adastra,[3] Antonina I. Frolova,[3] Maggie M. Chi,[3] Daniel Cusumano,[3] Mary Bade,[3] Mary O. Carayannopoulos,[5] and Kelle H. Moley[2,3,4]

[3]*Department of Obstetrics and Gynecology, Washington University School of Medicine, St. Louis, Missouri*
[4]*University of Medicine and Dentistry of New Jersey, New Brunswick, New Jersey*
[5]*Department of Cell Biology and Physiology, Washington University School of Medicine, St. Louis, Missouri*

ABSTRACT

SLC2A8, also known as GLUT8, is a facilitative glucose transporter expressed in the testis, brain, liver, heart, uterus, ovary, and fat. In this study we examined the effect of *Slc2a8* deficiency on mouse gamete, preimplantation embryo, and implantation phenotype, as well as postnatal growth and physiology. For this model, the transcriptional start site and exons 1–4 were targeted and a lack of protein expression was confirmed by Western immunoblot. Oocytes obtained from *Slc2a8*$^{-/-}$ mice demonstrated abnormal metabolism and ATP production. In addition, deletion of *Slc2a8* resulted in impaired decidualization, a critical step in the differentiation of endometrial stromal cells (ESCs), necessary for implantation. This indicates a role for SLC2A8 in decidualization, which is supported by *Slc2a8* mRNA expression in both mouse and human ESCs, which increases dramatically in response to hormonal changes occurring during the process of implantation. Ovarian transplantation studies confirm that lack of SLC2A8 affects both the embryo and the implantation processes. This phenotype leads to decreased litter size, and smaller pups at weaning that continue to display an abnormally small growth phenotype into adulthood. The *Slc2a8* null mice display decreased body fat by magnetic resonance imaging, and, interestingly, they are resistant to a diet high in fat and carbohydrates.

glucose homeostasis, glucose transport, GLUT8, growth, SLC2A8, uterine decidualization

INTRODUCTION

Glucose transporter 8 (SLC2A8) is a member of the class III of facilitative glucose transporters (SLC2As). All 14 known SLC2As have shared characteristics, including 12 transmembrane-spanning helices and an exofacial *N*-linked glycosylation site [1]; however, SLC2As are unique in tissue localization, kinetics, and substrate specificity. More specifically, SLC2A8 has a high affinity for glucose (Km ~2 mM), which can inhibit with fructose, galactose, and cytochalasin B, indicating that it may transport other hexoses [2].

SLC2A8 is expressed at high levels in the testis and is also found in brain, liver, heart, uterus, ovary, and fat [2, 3]. Furthermore, SLC2A8 is localized entirely intracellularly, except in blastocysts, where it has been shown to translocate to the plasma membrane in response to insulin stimulation [3, 4]. This intracellular localization is signaled by a dileucine motif (DE-XXXLL), which traffics SLC2A8 to the late endosome/lysosome [5]. Although research on this SLC2A is ongoing, a known function for the SLC2A8 remains elusive.

Our lab has previously indicated a role for SLC2A8 in preimplantation embryo survival in mice. Knockdown of *Slc2a*8 in the embryo, by antisense technology, resulted in an increase of apoptosis in blastocysts and a decrease in successful pregnancies by Day 14.5 [6]. These data, along with data indicating that SLC2A8 is translocated to the membrane in response to insulin in the blastocyst [3], suggest that SLC2A8 plays an important role in embryo development, possibly by facilitation of glucose utilization.

However, previously published *Slc2a8*-deficient models do not exhibit embryonic lethality, but do display a mild reproductive and behavioral phenotype. Membrez et al. [7] reported a mild brain phenotype consisting of increased proliferation of hippocampal cells and an increased P-wave duration in the heart. Another group described a phenotype in which deletion of *Slc2a8* resulted in reduced sperm motility and ATP and behavioral alterations, in particular hyperactivity [8, 9]. These phenotypes are not surprising, as SLC2A8 is highly expressed in the testes and also in the brain and heart. Both groups noted that the heterozygous mating of *Slc2a8* mice resulted in a lower than expected percentage of *Slc2a8*$^{-/-}$ and *Slc2a8*$^{+/-}$ pups, potentially resulting from the decreased motility observed in the sperm. Neither of these groups reported changes in normal glucose homeostasis or growth at baseline in these models.

In this paper we detail a distinct phenotype resulting from the creation of a *Slc2a8*-null mouse using a conventional knockout system, targeting the first four exons including the transcription start site. These mice exhibit a more severe reproductive phenotype than previous models, as litters born to *Slc2a8*$^{-/-}$ mating pairs are smaller in number than the wild-type controls (*Slc2a8*$^{+/+}$). A role for SLC2A8 in the metabolism of both female and male gametes is uncovered, as the sperm motility is decreased (which is attributed to decreased ATP levels previously [8]), and ATP levels in the oocyte are significantly decreased as well. Additionally, *Slc2a8*$^{-/-}$ females display a significant decrease in decidualization marker mRNA expression and exhibit incomplete decidualization of the uterus upon in vivo artificial stimulation, suggesting a role for SLC2A8 in the event of implantation and possibly placentation. Furthermore, in our model, SLC2A8 is required for normal growth, as *Slc2a8*$^{-/-}$ mice are smaller in size than their *Slc2a8*$^{+/+}$ counterparts. Finally, although SLC2A8 does not seem to be required for normal glucose homeostasis under basal conditions, removal of *Slc2a8* appears to protect the mice from the metabolic conditions induced by high-fat feeding.

[1]Supported by National Institutes of Health grant R01 HD40390 to K.H.M.
[2]Correspondence: Kelle H. Moley, 425 South Euclid Ave., Campus Box 8064, BJC Institute of Health, 10th Floor, St. Louis, MO 63110.
E-mail: moleyk@wustl.edu

Received: 16 November 2011.
First decision: 2 December 2011.
Accepted: 29 May 2012.

eISSN: 1529-7268 http://www.biolreprod.org
ISSN: 0006-3363

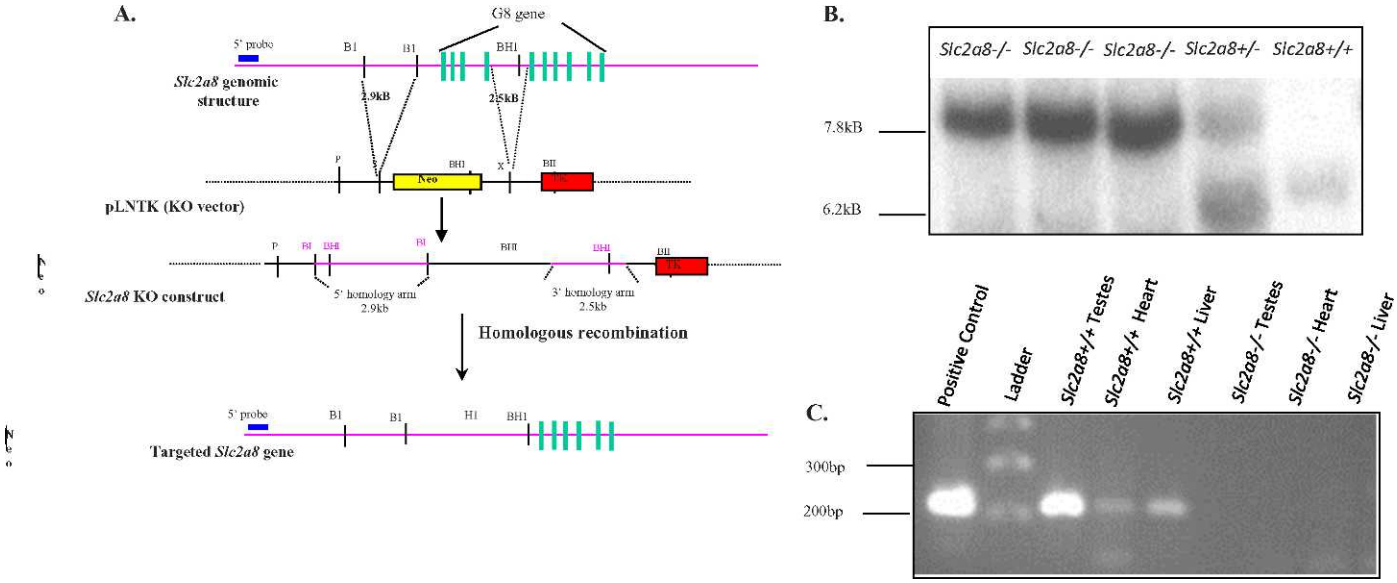

FIG. 1. Targeted disruption of *Slc2a8*. **A**) Schematic representation of the wild-type *Slc2a8* allele, the targeting vector used, the *Slc2a8* targeting construct, and the targeted *Slc2a8* gene are illustrated. Note the neomycin resistance gene replaces exons 1–4 of the *Slc2a8* gene. Additionally, the location of the external 5′ probe used to in Southern blot analysis of resistant ES clones and *Slc2a8*-deficient mice is indicated. BI, *Bgl*I; H, *Hind*III; BHI, *Bam*HI; P, *Pvu*I. **B**) Southern blot analysis of *Eco*RV-digested genomic tail DNA from the progeny of $Slc2a8^{+/-}$ mice. **C**) RT-PCR. Lane 1, positive control; lane 2, marker; lanes 3–5, $Slc2a8^{+/+}$ testes, heart, liver; lanes 6–8, $Slc2a8^{-/-}$ testes, heart, liver.

MATERIALS AND METHODS

Animal Care

All mouse studies were approved by the Animal Studies Committee at Washington University School of Medicine and conform to the *Guide for the Care and Use of Laboratory Animals* published by the National Institutes of Health.

Generation of Slc2a8 Targeting Construct

A P1 genomic clone generated from the 129 mouse strain was screened for the presence of *Slc2a8* by a commercial screening service (Genome Systems). Genomic DNA was prepared following the manufacturer's protocol and used as the template for generation of the *Slc2a8* targeting construct. A 2.9-kb BglI fragment was used for the 5′ arm (forward 5′-CACAAGGCCACATTGT-CAGCCCA-3′, reverse 5′-GCCGCGCTCGCCCGAGCGGC-3′) and a 2.5-kb PCR-generated fragment for the 3′ arm (forward 5′-GGGGGTTCCAGTG-CAAGGAAGGGTG-3′, reverse 5′-TCGTGGTACCGGTCATTC-3′) (Fig. 1A). The targeting vector (pLNTK) contains PGK-neo^r and HSV-TK genes for positive and negative selection, respectively.

Generation of Recombinant Slc2a8 Embryonic Stem Cell Clones and Southern Blot Analysis

RW4 embryonic stem (ES) cells (Washington University ES Core) were cultured on mitotically inactivated mouse embryonic fibroblasts (MEFs) in standard ES medium. ES cells were electroporated with 25 μg of linearized *Slc2a8* targeting vector and cultured on MEFs resistant to G418. After 24 h, the medium was supplemented with 400 μg/ml G418 (Gibco BRL), and resistant ES clones were isolated after 6 days of selection. Individual clones were expanded, and genomic DNA was prepared and analyzed by Southern blot analysis following established methods [10]. Briefly, genomic DNA was digested with *Eco*RV, resolved on 0.8% agarose gels, and transferred to nitrocellulose filters. Filters were hybridized with a 5′ external ^{32}P-labeled probe.

Western Blot

Protein was extracted from whole testes digest. The extracted protein was then run on 10% SDS-PAGE gel, transferred to nitrocellulose membrane, then blocked in 5% milk-Tris-buffered saline with Triton (TBS-T). Primary antibody specific to the C-terminal of *Slc2a8* (made by K.H.M., described previously [3]) was used at 1:1000 in 5% milk-TBS-T overnight at 4°C; goat anti-rabbit secondary was used at 1:10 000 in 1% milk/TBS-T for 1 h, washed, and developed by ECL (Amersham). The membrane was stripped and reprobed for actin (primary 1:10 000, secondary goat anti-mouse 1:10 000) as a loading control.

Computer-Assisted Sperm Analysis

The cauda epididymis was diced, and the sperm were allowed to disperse into the human tubal fluid (HTF) EmbryoMax (Millipore) for 10 min at 37°C. Motility parameters were measured by computer-assisted sperm analysis (CASA; Hamilton-Thorne Research).

Metabolic Analyses

Mice were primed with 10 IU equine chorionic gonadotropin by i.p. injection, and 48 h later cumulus-enclosed oocytes were obtained by manual rupturing of antral ovarian follicles. The ATP [11] and Hadh2 [12] microanalytic assays are described elsewhere. The assays were linked to NADPH. The NADPH by-product was then enzymatically amplified in a cycling reaction, and a byproduct of the amplification step was measured in a fluorometric assay.

Immunohistochemistry

Tissues were collected and fixed in 3% paraformaldehyde in PBS overnight at room temperature. The tissues were then dehydrated in serial dilution of ethanol and paraffin embedded. The tissues were sectioned and baked overnight at 56°C. For hematoxylin and eosin (H&E) staining, the tissues were deparaffinized in xylene for 5 min three times and rehydrated in serial dilutions of ethanol. After hydration in distilled water, the sections were stained with hematoxylin for 1 min and washed for 5 min in slowly running water. The sections were then counterstained with eosin for 30 sec and dehydrated in increasing concentrations of ethanol. After a 5-min treatment with xylene, the sections were air dried and mounted with a xylene-based mounting medium and viewed under a light microscope. For immunofluorescence staining, the tissue sections were treated with xylene for 20 min two times and then rehydrated in serial dilutions of ethanol. After washing with PBS, the sections were treated with 10 mM sodium citrate by boiling in the microwave. After cooling, the sections were washed in PBS and blocked in 5% normal serum in PBS/2% bovine serum albumin (BSA) for 1 h. Then the sections were incubated in the

primary antibody (1:100) in PBS/2% BSA overnight at 4°C (Cox2; Santa Cruz Biotechnology). The sections were washed three times in PBS/2% BSA and then incubated in secondary antibody (Alexa Fluor donkey anti-goat IgG 488; Molecular Probes) for 45 min at room temperature. The sections were rinsed three times again and treated with To-pro-3-iodide (1:500; Molecular Probes) in PBS for 15 min. After three more rinses in PBS, the coverslip was mounted using Vectashield (Vecta) and the sections were visualized by confocal microscopy.

RNA Isolation and Real-Time PCR

Total RNA was isolated using Trizol reagent (Invitrogen) and 1 μg RNA was reverse transcribed using the Quantitect Reverse Transcription kit (Qiagen). Quantitative RT-PCR was performed using SYBR green fluorescence and detected with the 7500 Fast Real-Time PCR System (Applied Biosystems). Each reaction was run in triplicate and consisted of 25 ng cDNA, 1x Fast Power SYBR Green PCR System (Applied Biosystems), and 300 nmM validated primers listed in Supplemental Table S1 (available online at www.biolreprod.org). The fold change in gene expression was calculated using the comparative cycle threshold method with the housekeeping gene, β-actin, as the internal control in murine cell studies.

Artificial Decidualization

To generate deciduomas, 7- to 8-wk-old female mice were used and treated as described previously [13]. Briefly, mice were ovariectomized and allowed 2 wk for recovery. They were then injected with 100 ng 17β-estradiol (E2) (Sigma) for 3 days, rested 2 days, and then injected with 10 ng of E2/1 μg of progesterone (P4) (Sigma) for 3 days. The steroids were diluted in sunflower seed oil (Sigma) and injections were all s.c., conducted at 1000–1030 h, with the total volume being 50 μl. Immediately after the last of the above sensitization injections, the right uterine horn received an intraluminal injection of 100 μl of sunflower seed oil. Mice continued to receive 1 mg of P4 s.c. for up to 4 days. On the day after the last injection the mice were killed and uterine horns dissected out and weighed.

Ovarian Transplant

Ten 8-wk-old mice in each group were used for the double ovarian transplant. Mice were anesthetized, and a small paralumbar incision in the lateral dorsal flanks was made, followed by a small incision in the peritoneal wall to allow access to the ovary. The ovary was removed from the bursa following an incision and kept in a culture dish of warm HTF medium. The surgical site was moistened with saline as needed. This procedure was conducted for a recipient mouse and the donor ovaries (of different genotype) were transplanted into the bursa of the mouse. The bursa tissue was closed and cauterized and the mouse was closed by suture. The donor mouse received the ovaries of the recipient mouse to complete the double ovarian transplant. The mice were allowed to recover 3 wk before they were placed in mating cages with males matching the genotype of the donated ovaries.

Glucose Tolerance and Insulin Tolerance Tests

Both of these methods were described elsewhere [14]. Briefly, for the glucose tolerance test (GTT), mice ($n = 10$ per group) were fasted 16 h prior to an oral gavage of 30% D-glucose (2 mg/g body wt; Sigma). Blood glucose was measured at 30-min intervals for 120 min via the tail vein blood on a Contour TS glucometer. For the insulin tolerance test (ITT), mice ($n = 10$ per group) were fasted 4 h prior to an intraperitoneal injection of bovine insulin (0.75 mU/g body weight; Sigma). Blood glucose was measured at 15-min intervals for 75 min via the tail vein. For the ITT, the percentage decreases in blood glucose from the 0-min time point was calculated.

High-Fat Diet

Beginning at age 4 wk, mice were fed a diet ad libitum consisting of either 58% fat (AIN-76A; Test Diet) or 4% fat standard control diet (5053; PicoLab) for a total of 12 wk. Mice were allowed free access to water and were maintained on a 12L:12D cycle. Mice were weighed weekly.

Statistical Analysis

All experiments were completed in triplicate. Data were analyzed using the Student *t*-test, and significance was reached at $P < 0.05$.

RESULTS

Generation of Slc2a8*-Deficient Mice*

Targeted disruption of the *Slc2a8* gene was accomplished via a *Slc2a8*-targeting construct designed to replace the first four exons, including the transcriptional start site and 200 bp of 5′ upstream sequence, of the *Slc2a8* gene with a neomycin resistance cassette (Fig. 1A). Genomic DNA isolated from a P1 clone screened for the presence of the *Slc2a8* gene was used as the template for the construct. The *Slc2a8* gene spans ~9 kb and consists of 10 exons [15]. Successful targeting was achieved by electroporation of ES cells with the linearized *Slc2a8* targeting construct and subsequent culture in the presence of G418. A total of 750 resistant clones were screened by Southern blot and 1 recombinant ES clone identified. A recombinant ES clone was microinjected into blastocysts of C57BL/6 mice. Chimeric mice were screened by Southern blot analysis and founders were intercrossed. Germline transmission of F1 offspring was confirmed by Southern blot analysis (Fig. 1B).

We also confirmed deletion of *Slc2a8* by RT-PCR in testes, heart, and liver tissues, which are all known to express *Slc2a8*. Although *Slc2a8* was detectable in these tissues in the wild-type animals, no expression was detectable in the testes, heart, and liver of $Slc2a8^{-/-}$ mice (Fig. 1C).

Impaired Protein Expression in Slc2a8*-deficient Mice*

To confirm that the deletion of the *Slc2a8* gene resulted in loss of protein expression, we performed Western blot and immunofluorescence analysis of testes. SLC2A8 is most abundantly expressed in the testes, in particular the spermatids, spermatozoa, and Leydig cells [16]. As illustrated in Figure 2A, SLC2A8 is present, as expected, in the $Slc2a8^{+/+}$ mice and transgenic global *Slc2a8*-overexpressed mice but is completely absent in testes from $Slc2a8^{-/-}$ mice. Furthermore, immunofluorescence staining of testes also confirmed the absence of SLC2A8 protein in the testes obtained from $Slc2a8^{-/-}$ mice (Fig. 2B). Upregulation of other facilitative glucose transporters SLC2A1 and SLC2A3 was not seen. These results confirm that successful deletion of *Slc2a8* was achieved and $Slc2a8^{-/-}$ mice are devoid of SLC2A8 protein.

Slc2a8$^{-/-}$ *Mice Mating Results in Smaller Litter Sizes*

Other mouse models deficient in *Slc2a8* display a reproductive phenotype with less than expected percentage of heterozygous and homozygous null mice obtained from heterozygous matings [7, 8]. One group determined that the sperm in their $Slc2a8^{-/-}$ mice was less motile than that of $Slc2a8^{+/+}$ mice as a result of decreased ATP and mitochondria membrane potential in the sperm [8]. Although the homozygous matings from their $Slc2a8^{-/-}$ mice produced smaller litters, they reported that this phenomenon was neither significant nor investigated. Our $Slc2a8^{-/-}$ mice exhibited a more severe reproductive phenotype, as litters that resulted from $Slc2a8^{-/-}$ mating were significantly smaller in number (average of four pups/litter) than litters from $Slc2a8^{+/+} \times Slc2a8^{+/+}$ matings (average of six pups/litter) (Table 1). To determine whether this phenotype was due to a male or female reproductive effect, we mated $Slc2a8^{-/-}$ males or females with their $Slc2a8^{+/+}$ counterparts. Interestingly, the matings resulted in a decreased number of pups similar to the numbers we observed in $Slc2a8^{-/-} \times Slc2a8^{-/-}$ matings. This suggests that these mice have a complex reproductive phenotype that may stem from an overarching phenotype. We will address these phenotypes individually in this paper.

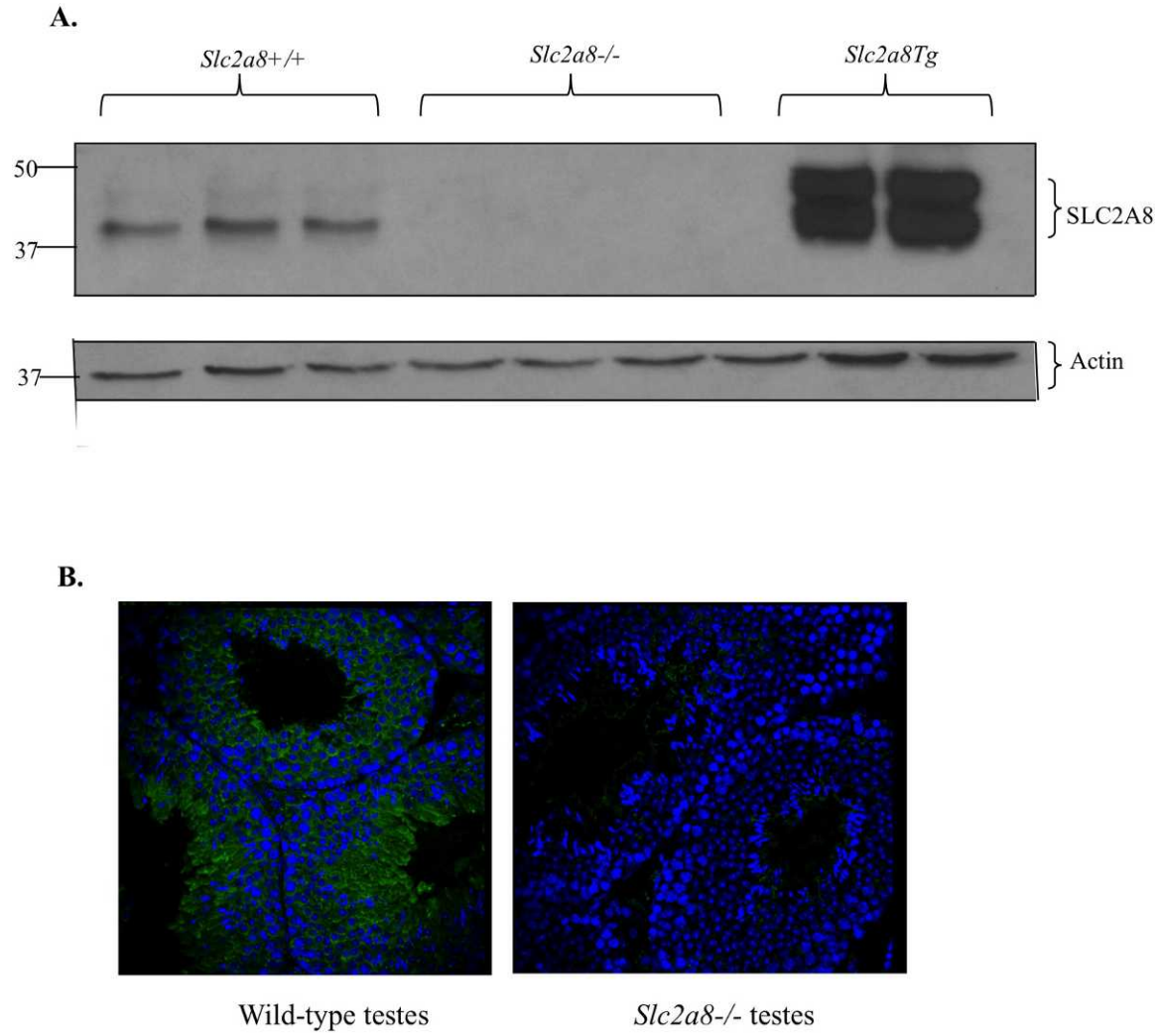

FIG. 2. Impaired protein expression in *Slc2a8*$^{-/-}$ mice. **A**) Western blot of SLC2A8 expression in testes protein. SLC2A8 is absent in testes from *Slc2a8*$^{-/-}$ mice. **B**) Immunofluorescence staining for SLC2A8 in paraffin-sectioned testes. SLC2A8 protein is not present in the *Slc2a8*$^{-/-}$ mice. Original magnification ×10.

Slc2a8$^{-/-}$ *Males Have Normal Testes Histology but Exhibit Reduced Sperm Motility*

SLC2A8 is most abundantly expressed in the testes in both mice and humans [2, 3]. Although the function of SLC2A8 is unknown, it has been previously suggested that SLC2A8 is important for energy metabolism in the sperm [16]. Using H&E staining, we examined the morphology of testes obtained from *Slc2a8*$^{-/-}$ compared to *Slc2a8*$^{+/+}$ mice. The overall morphology is normal and all cell types are present (Fig. 3A). In previously reported *Slc2a8*-deficient mice, no changes in morphology were observed, but the mice did exhibit a reduction in motility by CASA [8]. This reduction in motility is consistent with data indicating that SLC2A8 is localized mainly to the acrosome region, which is responsible for supplying the sperm with energy [16–18]. Therefore, we repeated this sperm motility assay using the *Slc2a8*$^{-/-}$ mice we generated (Fig. 3B). The mice did exhibit a reduction in motility, with a correlating low number of rapid sperm and an increased number of slow and static sperm; however, these data did not reach significance. Although there may be a trend towards a decrease in motility, this phenotype appears to be a minor factor contributing to the reduction in litter size observed.

Slc2a8$^{-/-}$ *Females Have Normal Ovarian Histology but an Abnormal Metabolic Profile*

We also examined the histology of the ovary, as the litter numbers obtained from our breeding crosses indicated a female reproductive phenotype as well. SLC2A8 is expressed in the tissues of the female reproductive tract, including the ovaries (and oocytes) and the uterus [19, 20]. The histology of ovaries from *Slc2a8*$^{-/-}$ mice was comparable to that of the *Slc2a8*$^{+/+}$ mice ovaries, and all cell types were present (Fig. 3C). Additionally, we sought to determine if the oocytes exhibited any metabolic disturbances as a result of being devoid of *Slc2a8*. Previous data from our lab and others have reported

TABLE 1. *Slc2a8*$^{-/-}$ mice displayed reduced litter sizes.

Male genotype	Female genotype	Pups per litter (average)	SEM	*P* value
Wild-type	Wild-type	6.0	2.2	—
Slc2a8$^{-/-}$	*Slc2a8*$^{-/-}$	4.3	1.7	0.00016
Wild-type	*Slc2a8*$^{-/-}$	3.7	1.7	0.0035
Slc2a8$^{-/-}$	Wild-type	4.4	1.9	0.0067
Slc2a8$^{+/-}$	*Slc2a8*$^{+/-}$	4	2	0.0029

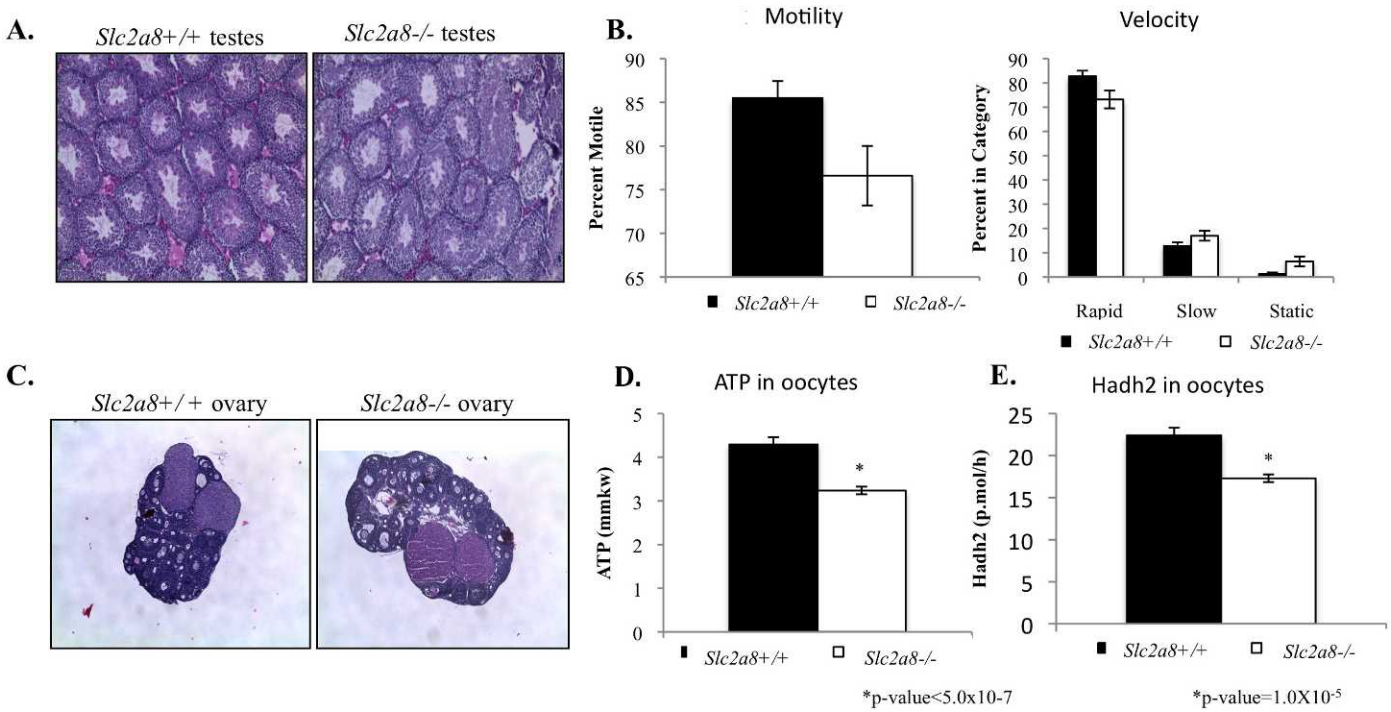

FIG. 3. Male and female gonadal phenotype. **A**) No changes in overall testes morphology observed in *Slc2a8*$^{-/-}$ mice. **B**) *Slc2a8*$^{-/-}$ mice exhibit a trend toward reduced sperm motility (n.s.). **C**) No changes in overall ovary morphology observed in *Slc2a8*$^{-/-}$ mice. **D**) ATP is significantly decreased in *Slc2a8*$^{-/-}$ oocytes by ~25%, n = 30. **E**) Hadh2 is significantly decreased in *Slc2a8*$^{-/-}$ oocytes by ~23%, n = 20. Original magnification ×4 (**A** and **C**). Error bars are ± SEM.

that glucose metabolism is critical to the process of meiosis in the oocyte [11, 21, 22]. A dysregulation of glucose metabolism leading to a decrease in ATP production results in oxidative stress and overall poorer outcomes in oocyte development [23, 24]. Using a microanalytic technique in which we can measure the metabolites of a single oocyte, we determined that the ATP content in *Slc2a8*$^{-/-}$ oocytes was significantly decreased compared to that of *Slc2a8*$^{+/+}$ oocytes (~25% less; Fig. 3D). These data were similar to reported metabolic abnormalities in oocytes obtained from diabetic mice and older human patients undergoing IVF [11, 25].

To further profile these metabolic abnormalities, we examined an important enzyme in fatty acid metabolism, hydroxyacyl-CoA dehydrogenase or Hadh2 (formerly BOAC). Our results indicate a decrease in Hadh2 activity in oocytes obtained from *Slc2a8*$^{-/-}$ mice compared to oocytes from wild-type mice (Fig. 3E). In humans, a decrease in this enzyme indicates a poorer-quality oocyte [25]. Our lab has also published results indicating a decrease in this enzyme in oocytes from diabetic mice along with a decrease in ATP due to a decrease in AMPK. This metabolic profile results in a poorer-quality oocyte [11]. Furthermore, it has been hypothesized that Hadh2 is critical to blastocyst development, as the acyl-CoA dehydrogenase null mouse is embryonic lethal at the morula-to-blastocyst transition [26].

Therefore, we concluded that although overall morphology of the ovary was normal, oocytes obtained from *Slc2a8*$^{-/-}$ mice exhibited abnormalities in metabolic pathways potentially resulting in a poorer-quality oocyte and contributing to the reduced litter size seen among the *Slc2a8*$^{-/-}$ mice.

In Vivo Uterine Decidualization Is Affected in Slc2a8$^{-/-}$ *Mice*

SLC2A8 is expressed in the uterus of both mice and humans. Expression in the whole uterus, including the stroma, the decidua, and both the luminal and glandular epithelium, has been reported [20]. Although our lab has previously confirmed the necessity of SLC2A1 in uterine decidualization, mRNA expression of SLC2A8 is dramatically increased upon embryo implantation and decidualization in both mice and humans, indicating that it may play an important role in this process as well [19]. Therefore, in order to determine whether reduced litter size of the *Slc2a8*$^{-/-}$ mice is due to aberrant decidualization, we investigated this process in the *Slc2a8*$^{-/-}$ mice.

The process of decidualization is initiated by the implantation of the blastocyst on Day 4.5 in mice. The uterus, in particular the stromal cells of the endometrium, will undergo a series of events both morphologically and biochemically, creating a distinct populations of decidualized cells, which support the implanting embryo. To investigate this process in vivo, we mated the mice and collected implantation sites on Day 6.5. These sites either were examined for morphology or were examined for decidualization markers by quantitative real-time PCR (qPCR). In order to investigate morphology, we stained the sections with H&E (Fig. 4, A and B). Observations of the sections suggested a smaller area of decidualization in the *Slc2a8*$^{-/-}$ uterus. This was confirmed by immunofluorescence staining of the Day 6.5 sections with *Cox2*, a known decidualization marker, as we observed a decreased expression of *Cox2* (Fig. 4, C–E).

In order to examine this apparent change in decidualization in our *Slc2a8*$^{-/-}$ mice, we used qPCR to determine mRNA expression levels of two known decidualization markers, cyclooxygenase 2 (*Cox2*) and prolactin-related protein (*Prp*), in Day 6.5 implantation sites from *Slc2a8*$^{-/-}$ mice and compared them to wild-type implantation sites (Fig. 4, F and G). Expression levels of *Cox2* and *Prp* were significantly reduced in the Day 6.5 implantation sites from *Slc2a8*$^{-/-}$ mice compared to wild-type levels. This decrease in mRNA

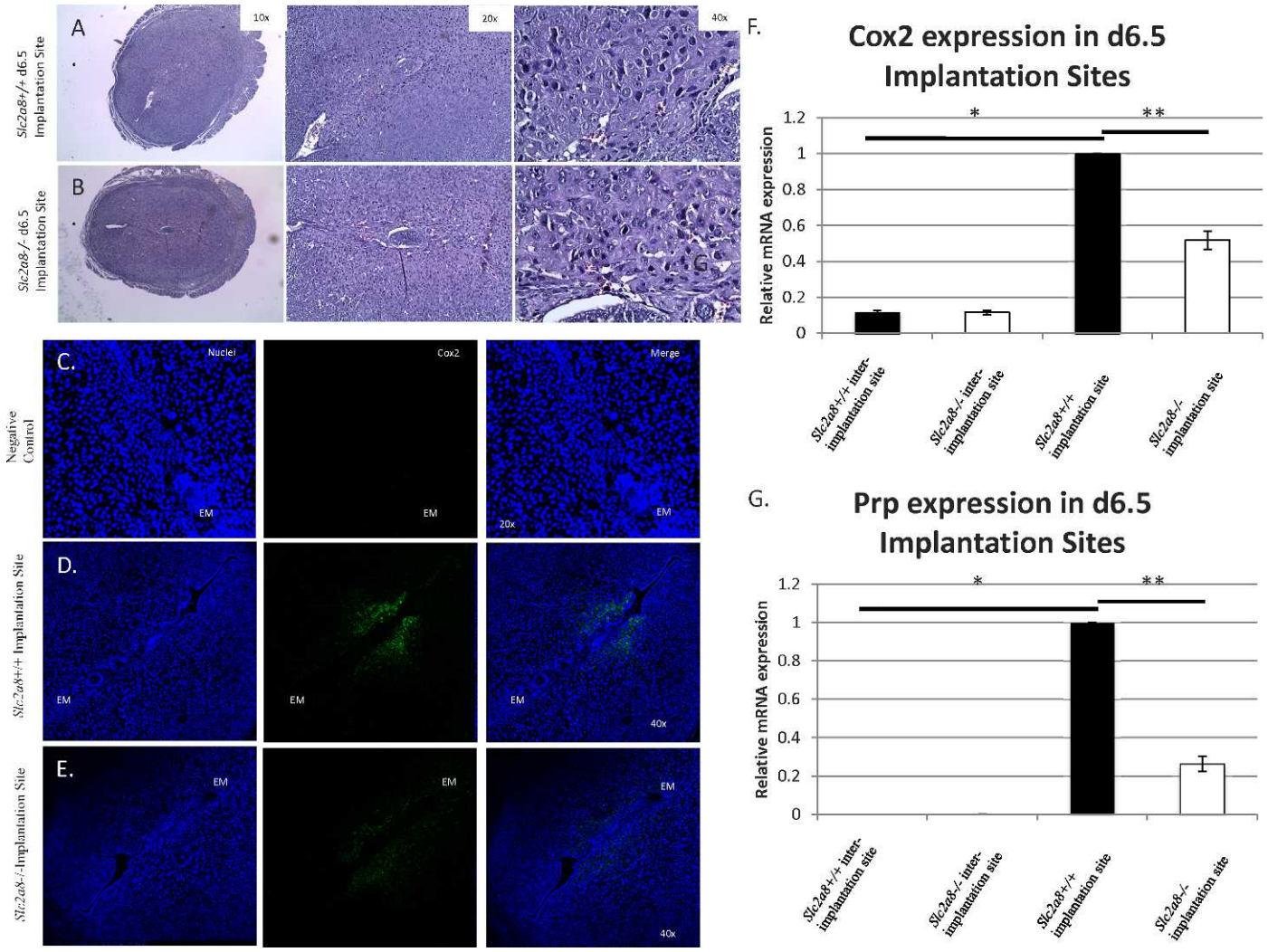

FIG. 4. Aberrant uterine decidualization in *Slc2a8*$^{-/-}$ mice. H&E staining of Day 6.5 implantation sites in wild-type (**A**) and *Slc2a8*$^{-/-}$ mice (**B**). Immunofluorescence staining of Cox2 in Day 6.5 implantation sites; the site of the implanted embryo is marked as EM. Negative control (**C**), wild-type (**D**), *Slc2a8*$^{-/-}$ (**E**). Quantitative real-time of wild-type and *Slc2a8*$^{-/-}$ Day 6.5 implantation sites for *Cox2* (**F**) and *Prp* (**G**). Interimplantation areas were excised and used for negative control. $*P < 1.0 \times 10^{-6}$; $**P < 0.001$. Error bars are ± SEM.

expression indicated that lack of *Slc2a8* was leading to a reduction in decidualization.

However, it was not clear whether this aberrant decidualization was due to hormonal regulation or even embryonic effects. Therefore, we used a rodent-specific in vivo artificial decidualization technique in which we ovariectomized the mice and supplemented hormonal stimuli by subcutaneous injection of E2 and P4 [13]. Using this method, we were able to decidualize the uterus in vivo controlling for hormonal stimuli and in the absence of an embryo, allowing for examination of the uterus without the interference of the embryo or ovarian effects.

The *Slc2a8*$^{-/-}$ mice had observably smaller decidualized horns compared to the *Slc2a8*$^{+/+}$ mice (Fig. 5A). Moreover, the mass of the decidualized horn compared to the internal control was significantly smaller when compared to the *Slc2a8*$^{+/+}$ counterparts (~35% less; Fig. 5B). This confirmed the decrease in decidualization in the *Slc2a8*$^{-/-}$ mice. This aberration in decidualization may have led to the smaller litter numbers obtained in the breeding crosses due to abnormal implantation.

However, given the abnormal metabolic profile and lower ATP levels exhibited in *Slc2a8*$^{-/-}$ gametes, it is possible that lack of *Slc2a8* in the embryo may have contributed to the reduction in litter sizes. This is supported by our previous report of *Slc2a8* knockdown by antisense technology, which led to increased apoptosis and decreased pregnancy rates. Therefore, to address the embryonic and uterine effects separately, we conducted double ovarian transplants, in which we transplanted ovaries from either wild-type or *Slc2a*$^{-/-}$ mice into the contrary genetic counterpart. Using this method, we were able to separate the potential embryonic phenotype (from the affected gamete metabolism) from the aberrant uterine decidualization we observed as we investigated *Slc2a8*$^{-/-}$ embryos in a wild-type uterus and wild-type embryos in an *Slc2a8*$^{-/-}$ uterus. The resultant females were mated with males matching their ovarian genotype; a cartoon representing the outcome of the matings is presented in Figure 6A. The litter sizes of these resultant crosses were recorded and the results are shown in Figure 6B. Interestingly, both groups showed a reduction in litter size similar to that of the *Slc2a8*$^{-/-}$ homozygous matings, indicating that the loss of pups may

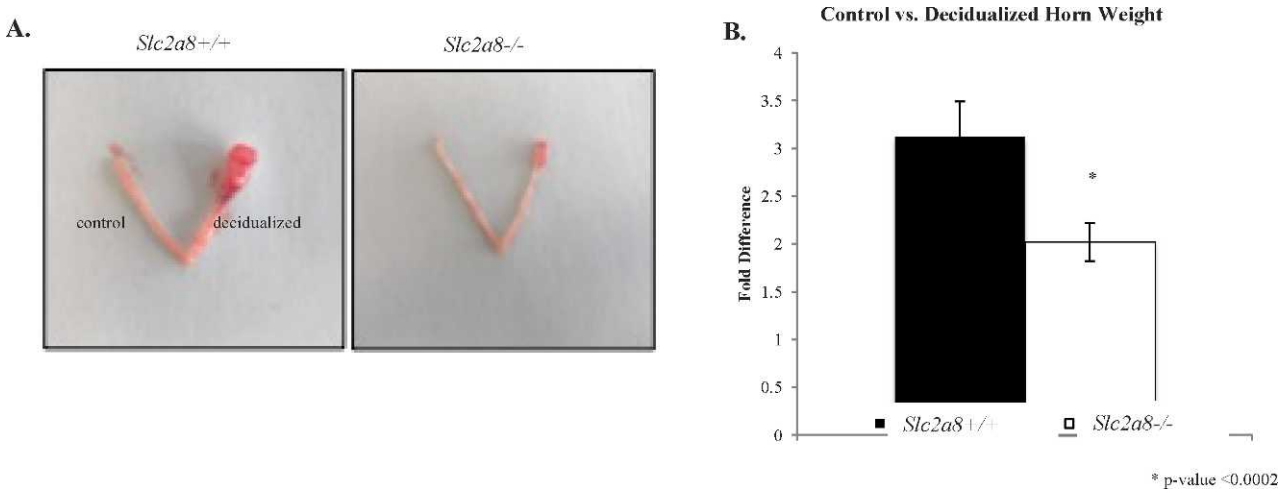

FIG. 5. In vivo artificial decidualization is incomplete in *Slc2a8*$^{-/-}$ mice. **A**) Representative image of control horn (left) and deciduoma (right) in the *Slc2a8*$^{+/+}$ (left) and *Slc2a8*$^{-/-}$ (right) uterus. **B**) The *Slc2a8*$^{-/-}$ decidualized horn weighed significantly less than the *Slc2a*$^{+/+}$ decidualized horn compared to control horns. Error bars are ± SEM.

have been contributed to by both embryonic and uterine factors.

Slc2a8$^{-/-}$ *Mice Weigh Significantly Less than* Slc2a8$^{+/+}$ *Mice*

Although other groups have reported no overall change in whole glucose homeostasis in mice deficient in SLC2A8, our *Slc2a8*$^{-/-}$ mice were observably smaller than their *Slc2a8*$^{+/+}$ counterparts at the time of weaning. The graph in Figure 7A, details weights of the mice starting at 3 wk of age until 8 wk of age. The *Slc2a8*$^{-/-}$ mice started out significantly smaller than the *Slc2a8*$^{+/+}$ mice at weaning and continued to be smaller despite maturation into adulthood.

To determine whether the mice exhibited this small size phenotype starting at birth, we weighed the pups at Postnatal Day 1. The pup sizes were not significantly different between the two groups (Fig. 7B), suggesting that this phenotype manifests later in life. Next, we examined the daily food intake of these mice to determine if a difference in food consumption was responsible for the smaller size phenotype. The *Slc2a8*$^{-/-}$ mice consumed a similar amount of food (in grams) to the *Slc2a8*$^{+/+}$ over several weeks (Fig. 7C). Finally, we investigated the body composition and fat storage and distribution by gonadal fat pad weight and by body fat percentage using magnetic resonance imaging (MRI). The gonadal fat pad was smaller (not shown) and the body fat percentage by MRI was similarly less; however neither of these numbers reached significance (Fig. 8A).

Our results indicated that lack of SLC2A8 during development resulted in a smaller body size, starting with differences observed at weaning. These differences resulted in a decrease in body fat, although not a significant decrease, and were not attributed to food intake.

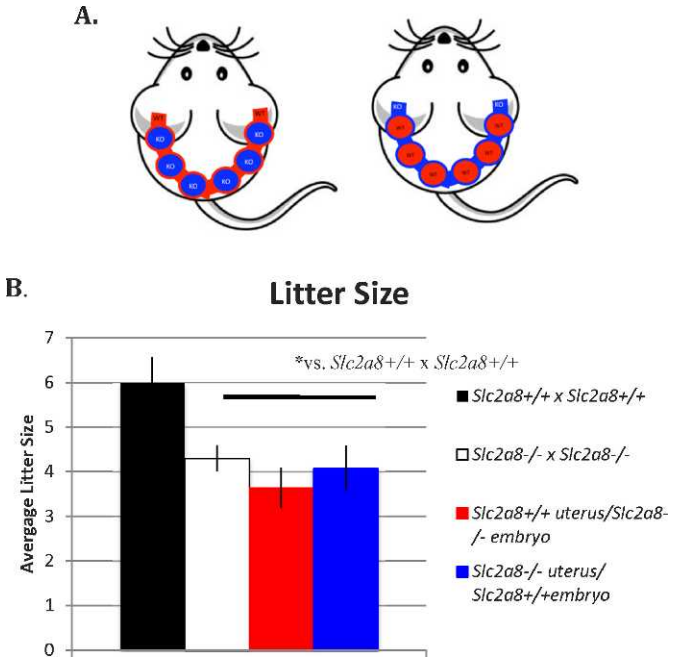

FIG. 6. Ovarian transplants result in reduced litter sizes. **A**) Cartoon depicting experimental overview. **B**) Compared to wild-type × wild-type matings, both groups of mice who underwent the ovarian transplant show decreased number of pups per litter similar to *Slc2a8*$^{-/-}$ × *Slc2a8*$^{-/-}$ matings. Error bars are ± SEM.

Slc2a8$^{-/-}$ *Mice Do Not Exhibit a Change in Whole-Body Glucose Homeostasis*

In order to test whether a dysregulation of whole-body glucose homeostasis was contributing to the smaller size phenotype observed in the *Slc2a8*$^{-/-}$ mice, we completed both GTTs and ITTs. The literature suggests that SLC2A8 is not critical in maintaining whole-body glucose homeostasis at the basal state. Both tests exhibited clearance results similar to those of *Slc2a8*$^{+/+}$ mice (Fig. 8, B and C). Therefore, our data also suggested that *Slc2a8*$^{-/-}$ does not play a role in whole-body glucose homeostasis under basal conditions.

Slc2a8$^{-/-}$ *Mice Are Resistant to a High-Fat Diet*

Although SLC2A8 did not appear to be critical to overall whole-body glucose homeostasis during basal conditions, we noticed a distinct phenotype when the mice were fed a diet high in fat and carbohydrates (58%) compared to a control diet (4%). We fed Slc2a8$^{-/-}$ and wild-type mice either the control

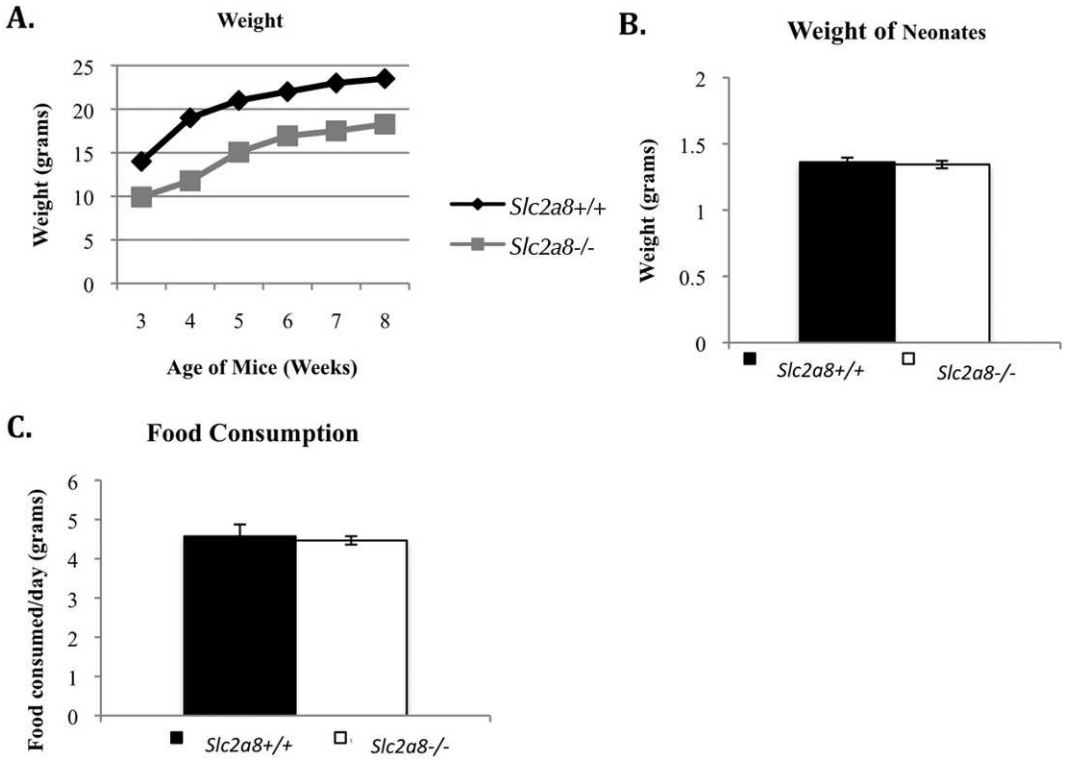

FIG. 7. *Slc2a8*$^{-/-}$ mice exhibit aberrant growth. **A**) *Slc2a8*$^{-/-}$ mice are smaller at 3 wk of age and into adulthood. Male mice are shown but females exhibit the same pattern. **B**) Weights of pups at Postnatal Day 1 are similar to those of *Slc2a8*$^{+/+}$ mice. **C**) *Slc2a8*$^{-/-}$ mice consume the same amount of food as *Slc2a8*$^{+/+}$, indicating this is not related to a decrease in calorie consumption. Error bars are ± SEM.

or high-fat diet for a total of 12 wk and then completed a regimen of assays to determine the response of the mice. We found that the *Slc2a8*$^{-/-}$ mice did not gain as much weight on the diet as the *Slc2a8*$^{+/+}$ mice (Fig. 8D). This could be attributed to a lack of body fat stores, as the *Slc2a8*$^{-/-}$ mice exhibited significantly less body fat by MRI (Fig. 8D). Moreover, the *Slc2a8*$^{-/-}$ mice fed the high-fat diet exhibited improved glucose clearance at 60 min during the GTT (Fig. 8E), as well as a normal ITT, as compared to the *Slc2a8*$^{+/+}$ fed a high-fat diet (Fig. 8F). This suggests that the *Slc2a8*$^{-/-}$ mice were more resistant to the effects of a diet high in fats and sugars compared to controls. The mechanism is not clear; however, recent studies by our lab indicate that expression of SLC2A8 may be influencing the expression of other SLC2As in the gut.

DISCUSSION

SLC2A8 is expressed in insulin-sensitive tissues such as brain and muscle as well as in other tissues such as ovary, uterus, liver, and heart, and it is most highly expressed in the testes [2, 3]. Interestingly, unlike other transporters, which either reside at the plasma membrane (i.e., SLC2A1) or are shuttled there (i.e., SLC2A4), SLC2A8 is found intracellularly, with reported localization in the membranes of late endosomes/lysosomes and of the endoplasmic reticulum in the brain [5, 27]. One exception to this localization pattern is in the murine blastocyst, where SLC2A8 can be triggered to translocate to the plasma membrane in response to insulin [3]. Although two papers have reported models of *Slc2a8*-deficient mice, the function of this unique transporter remains elusive.

Using conventional knockout strategies, we generated *Slc2a8*$^{-/-}$ mice that exhibited a reproductive phenotype resulting in a significant decrease in the number of pups per litter. The *Slc2a8*$^{-/-}$ mating pairs displayed 30% fewer mice per litter as compared to *Slc2a8*$^{+/+}$ pairs (Table 1). This phenotype is more severe than that previously described in other *Slc2a8*-deficient models. This disparity could be due to the fact that one conditional knockout was made with a *Nestin* cre-knockout model, or due to strain differences or some yet uncovered overarching phenotype in the *Slc2a8* null mice.

In order to investigate the reproductive phenotype, we examined both gonadal and gestational characteristics in the mice. The male mice exhibited overall normal testes morphology; however, the sperm were less motile (n.s., not significant) (Fig. 3, A and B). This finding is supported by previously published models, in which deletion of *Slc2a8* resulted in lower ATP in the sperm, leading to a decrease in sperm motility [8]. Next, we examined the ovaries of the female mice. Again, overall, the morphology was similar to that of the wild type; however, ATP levels were significantly (25%) lower in the *Slc2a8*-null oocytes compared to wild-type (Fig. 3, C and D). This discrepancy, along with a decrease in Hadh2, indicates aberrant energy metabolism in the gonad. Changes in energy metabolism and in particular in ATP have been associated with poorer-quality gametes, which lead to unfavorable embryonic outcomes [23, 24, 28]. The reason for this difference in the *Slc2a8*$^{-/-}$ oocytes is not clear but may be related to a decrease in glucose uptake in the COC [29].

The process of uterine decidualization is a glucose-dependent process, which is mediated mainly by SLC2A1 [19, 30]. However, previously our lab has detailed the significant upregulation of *Slc2a8* expression in decidualized uterine cells in both mice and humans [19]. Examination of the decidualization process in Slc2a8$^{-/-}$ mice suggests that SLC2A8 is required for complete decidualization. Using

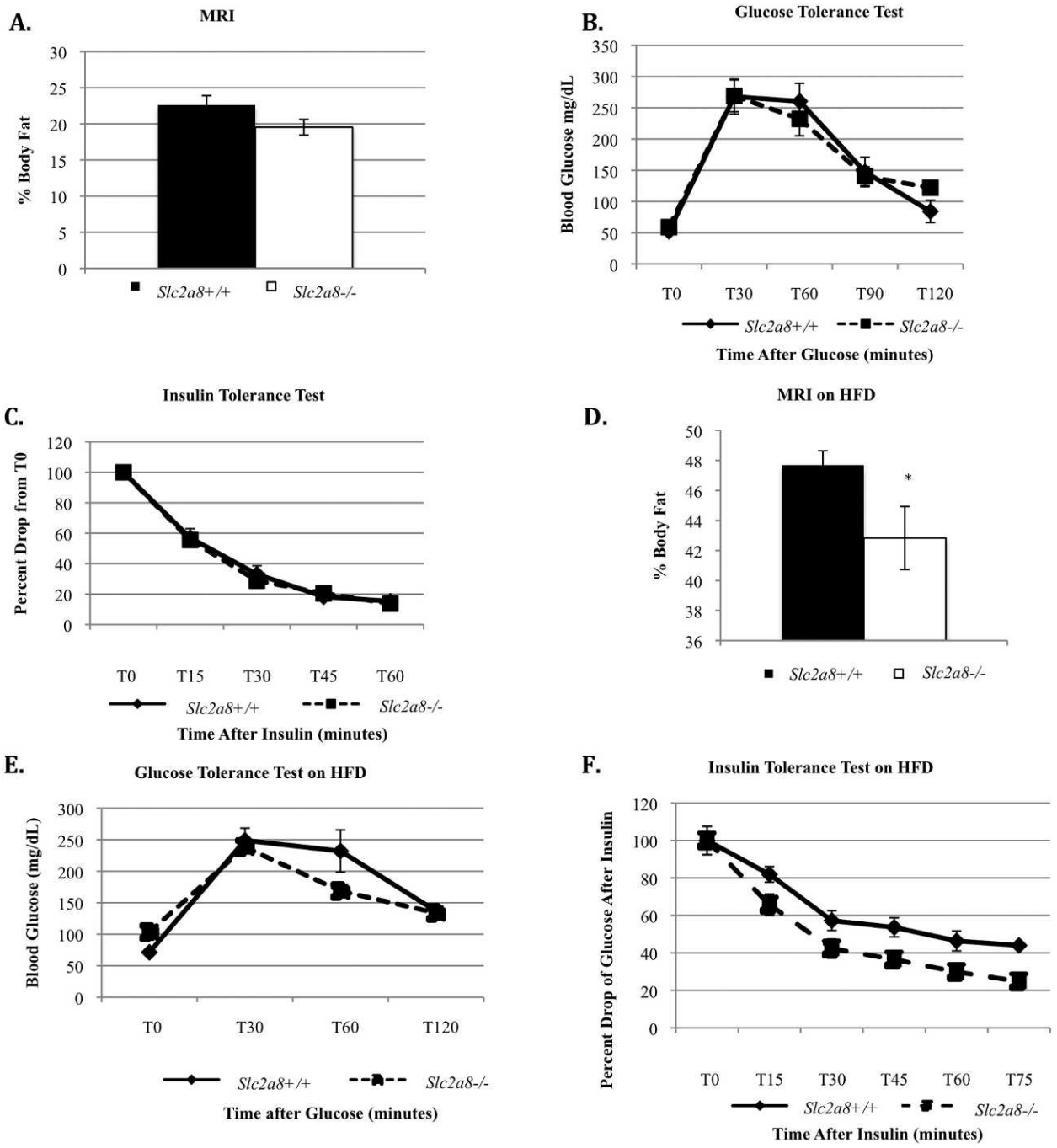

FIG. 8. Overall glucose homeostasis is not affected under normal conditions and maintained during high-fat feedings. **A**) *Slc2a8*$^{-/-}$ mice have less body fat by magnetic resonance imaging than *Slc2a8*$^{+/+}$ mice (n.s.). **B** and **C**) GTTs and ITTs are similar to those of *Slc2a8*$^{+/+}$ mice. **D**) *Slc2a8*$^{-/-}$ mice do not gain significant body fat on a high-fat diet compared to *Slc2a8*$^{+/+}$ mice. **E** and **F**) *Slc2a8*$^{-/-}$ mice maintain a normal GTT and ITT on a high-fat diet. Error bars are ± SEM.

known decidualization markers, *Cox2* and *Prp*, we report a decrease in mRNA expression of these markers in *Slc2a8*$^{-/-}$ implantation sites, indicating a lack of decidualization (Fig. 4, F and G). To verify this hypothesis, we used a rodent-specific artificial decidualization technique, which confirmed that the *Slc2a8*$^{-/-}$ mice do appear to exhibit an incomplete decidualization of the uterus (Fig. 5, A and B), as demonstrated by a lack of artificial decidualization in the mice. Although the role for SLC2A8 in uterine decidualization is not clear, SLC2A8 contains a targeting motif, which directs it to the lysosome in most of the tissues studied. The role of SLC2A8, therefore, may represent a lysosomal hexose transport facilitating the recycling of sugars during processes requiring an abundance of energy, such as decidualization. Disruption of SLC2A8 expression may explain the reproductive failures as a function of the poor implantation of embryos leading to a decrease in successful pups per pregnancy.

In conclusion, the *Slc2a8*-deficient mice generated by our lab display a more severe reproductive phenotype then previously reported in other models, leading to a smaller

litter size. This difference may be due to the fact that the first null model was a *Nestin*-cre and the second mouse still produced a truncated version of the SLC2A8 protein [7–9]. We attribute our reproductive findings to potentially both a gonadal and uterine phenotype. The gametes exhibit abnormal energy metabolism in both previous reported findings and in our study, in which the oocytes have lower ATP levels. Furthermore, we have found a disruption in the uterine decidualization process. Although these findings are novel, there may be an overarching phenotype, which is not yet elucidated in the SLC2A8 mice we have generated, such as a hormonal dysregulation.

Although previous *Slc2a8*-deficient mice models have had no growth disturbances, our *Slc2a8*-deficient mice reveal a need for SLC2A8 in normal growth, as the mice are smaller than their wild-type counterparts at 3 wk of age and into adulthood (in both sexes) (Fig. 7A). However, this growth phenotype is not associated with a dysregulation of overall whole-body glucose homeostasis, as the ability to clear glucose/insulin is similar to that of wild-type mice (Fig. 8, B and C). Furthermore, this small size phenotype is not attributed to an increase in food intake, as the mice eat similar amounts of food to the wild-type mice (Fig. 7C).

Although SLC2A8 does not appear to be necessary for normal whole-body glucose homeostasis, other SLC2As may be compensating for SLC2A8, masking a role for this transporter. Therefore, we were interested in whether stressing the mice would uncover a role for SLC2A8 in this process. We fed the mice a high-fat, high-carbohydrate diet for 12 wk and assayed the mice for changes in glucose homeostasis. After 12 wk on the diet, the *Slc2a8*-deficient mice exhibited significantly less body fat than the wild-type mice (Fig. 8D). And interestingly, *Slc2a8*-deficient mice appeared to have an improved glucose clearance compared to wild-type, as a GTT revealed (Fig. 8E). Additionally, an ITT performed after 12 wk on the diet showed comparable insulin tolerance to mice on normal chow (Fig. 8F). Further studies to determine the reasons for these differences will need to be completed in the future. It is possible that other SLC2As are upregulated in response to the deletion of *Slc2a8* or that there is a function for SLC2A8 that is yet to be elucidated leading to these findings.

In conclusion, *Slc2a8*-deficient mice are smaller at 3 wk of age but exhibit a normal glucose homeostasis on normal chow despite a smaller growth trajectory as compared to controls that extends into adulthood. However, when the mice are fed a diet consisting of high fat and high carbohydrate, the mice appear resistant to the deleterious effects of this diet, observed in the wild-type mice. Therefore, we conclude that SLC2A8 is important in normal growth. Although both the reproductive and growth phenotype are novel and distinct, we believe that there may be an overall disruption of energy metabolism during development, which explains our observations. It is possible that SLC2A8 is present in lysosomal membranes to transport and thus recycle glucose residues from degraded glycosylation sites on proteins targeted for autophagy or lysosomal degradation. This function may be critical in processes that require an abundance of glucose (and SLC2A8 is shown to be increased), such as uterine decidualization and fat differentiation [19, 20, 27, 30, 31], and thus lack of SLC2A8 expression globally accounts for abnormal decidualization and possibly subsequent placentation and fetal growth, as well as differentiation of adipose cells, thus accounting for elimination of lipid accumulation and fat pad mass in the knockout mice. Further studies, however, will need to be completed to fully understand the role of SLC2A8.

ACKNOWLEDGMENT

The authors would like to acknowledge the NORC for use of the MRI supported by grant P30DK056341 and the Developmental Biology Histology & Microscopy Core for tissue sectioning.

REFERENCES

1. Augustin R. The protein family of glucose transport facilitators: it's not only about glucose after all. IUBMB Life 2010; 62:315–333.
2. Ibberson M, Uldry M, Thorens B. GLUTX1, a novel mammalian glucose transporter expressed in the central nervous system and insulin-sensitive tissues. J Biol Chem 2000; 275:4607–4612.
3. Carayannopoulos MO, Chi MM, Cui Y, Pingsterhaus JM, McKnight RA, Mueckler M, Devaskar SU, Moley KH. GLUT8 is a glucose transporter responsible for insulin-stimulated glucose uptake in the blastocyst. Proc Natl Acad Sci U S A 2000; 97:7313–7318.
4. Diril MK, Schmidt S, Krauss M, Gawlik V, Joost HG, Schurmann A, Haucke V, Augustin R. Lysosomal localization of GLUT8 in the testis–the EXXXLL motif of GLUT8 is sufficient for its intracellular sorting via AP1- and AP2-mediated interaction. FEBS J 2009; 276:3729–3743.
5. Augustin R, Riley J, Moley KH. GLUT8 contains a [DE]XXXL[LI] sorting motif and localizes to a late endosomal/lysosomal compartment. Traffic 2005; 6:1196–1212.
6. Pinto AB, Carayannopoulos MO, Hoehn A, Dowd L, Moley KH. Glucose transporter 8 expression and translocation are critical for murine blastocyst survival. Biol Reprod 2002; 66:1729–1733.
7. Membrez M, Hummler E, Beermann F, Haefliger JA, Savioz R, Pedrazzini T, Thorens B. GLUT8 is dispensable for embryonic development but influences hippocampal neurogenesis and heart function. Mol Cell Biol 2006; 26:4268–4276.
8. Gawlik V, Schmidt S, Scheepers A, Wennemuth G, Augustin R, Aumuller G, Moser M, Al-Hasani H, Kluge R, Joost HG, Schurmann A. Targeted disruption of Slc2a8 (GLUT8) reduces motility and mitochondrial potential of spermatozoa. Mol Membr Biol 2008; 25:224–235.
9. Schmidt S, Gawlik V, Holter SM, Augustin R, Scheepers A, Behrens M, Wurst W, Gailus-Durner V, Fuchs H, Hrabe de Angelis M, Kluge R, Joost HG, et al. Deletion of glucose transporter GLUT8 in mice increases locomotor activity. Behav Genet 2008; 38:396–406.
10. Sambrook J, Russell DW. Molecular Cloning: A Laboratory Manual. Cold Spring Harbor, NY: Cold Spring Harbor Laboratory Press; 2001.
11. Ratchford AM, Chang AS, Chi MM, Sheridan R, Moley KH. Maternal diabetes adversely affects AMP-activated protein kinase activity and cellular metabolism in murine oocytes. Am J Physiol Endocrinol Metab 2007; 293:E1198–E1206.
12. Lowry OH, Berger SJ, Carter JG, Chi MM, Manchester JK, Knor J, Pusateri ME. Diversity of metabolic patterns in human brain tumors: enzymes of energy metabolism and related metabolites and cofactors. J Neurochem 1983; 41:994–1010.
13. Frolova AI, O'Neill K, Moley KH. Dehydroepiandrosterone inhibits glucose flux through the pentose phosphate pathway in human and mouse endometrial stromal cells, preventing decidualization and implantation. Mol Endocrinol 2011; 25:1444–1455.
14. Purcell SH, Aerni-Flessner LB, Willcockson AR, Diggs-Andrews KA, Fisher SJ, Moley KH. Improved insulin sensitivity by GLUT12 overexpression in mice. Diabetes 2011; 60:1478–1482.
15. Scheepers A, Doege H, Joost HG, Schurmann A. Mouse GLUT8: genomic organization and regulation of expression in 3T3-L1 adipocytes by glucose. Biochem Biophys Res Commun 2001; 288:969–974.
16. Kim ST, Moley KH. The expression of GLUT8, GLUT9a, and GLUT9b in the mouse testis and sperm. Reprod Sci 2007; 14:445–455.
17. Gomez O, Romero A, Terrado J, Mesonero JE. Differential expression of glucose transporter GLUT8 during mouse spermatogenesis. Reproduction 2006; 131:63–70.
18. Schurmann A, Axer H, Scheepers A, Doege H, Joost HG. The glucose transport facilitator GLUT8 is predominantly associated with the acrosomal region of mature spermatozoa. Cell Tissue Res 2002; 307: 237–242.
19. Frolova AI, Moley KH. Quantitative analysis of glucose transporter mRNAs in endometrial stromal cells reveals critical role of GLUT1 in uterine receptivity. Endocrinology 2011; 152:2123–2128.
20. Kim ST, Moley KH. Regulation of facilitative glucose transporters and AKT/MAPK/PRKAA signaling via estradiol and progesterone in the mouse uterine epithelium. Biol Reprod 2009; 81:188–198.
21. Downs SM, Humpherson PG, Leese HJ. Meiotic induction in cumulus cell-enclosed mouse oocytes: involvement of the pentose phosphate pathway. Biol Reprod 1998; 58:1084–1094.

22. Sutton-McDowall ML, Gilchrist RB, Thompson JG. The pivotal role of glucose metabolism in determining oocyte developmental competence. Reproduction 2010; 139:685–695.
23. Van Blerkom J, Davis PW, Lee J. ATP content of human oocytes and developmental potential and outcome after in-vitro fertilization and embryo transfer. Hum Reprod 1995; 10:415–424.
24. Guerin P, El Mouatassim S, Menezo Y. Oxidative stress and protection against reactive oxygen species in the pre-implantation embryo and its surroundings. Hum Reprod Update 2001; 7:175–189.
25. Yazigi RA, Chi MM, Mastrogiannis DS, Strickler RC, Yang VC, Lowry OH. Enzyme activities and maturation in unstimulated and exogenous gonadotropin-stimulated human oocytes. Am J Physiol 1993; 264: C951–955.
26. Berger PS, Wood PA. Disrupted blastocoele formation reveals a critical developmental role for long-chain acyl-CoA dehydrogenase. Mol Genet Metab 2004; 82:266–272.
27. Schmidt S, Joost HG, Schurmann A. GLUT8, the enigmatic intracellular hexose transporter. Am J Physiol Endocrinol Metab 2009; 296:E614–618.
28. Menezo Y, Guerin P. Gamete and embryo protection against oxidative stress during medically assisted reproduction [in French]. Bull Acad Natl Med 2005; 189:715–726; discussion 726–718.
29. Purcell SH, Chi MM, Moley KH. Insulin-stimulated glucose uptake occurs in specialized cells within the cumulus oocyte complex. Endocrinology 2012; 153:2444–2454.
30. Frolova A, Flessner L, Chi M, Kim ST, Foyouzi-Yousefi N, Moley KH. Facilitative glucose transporter type 1 is differentially regulated by progesterone and estrogen in murine and human endometrial stromal cells. Endocrinology 2009; 150:1512–1520.
31. von Wolff M, Ursel S, Hahn U, Steldinger R, Strowitzki T. Glucose transporter proteins (GLUT) in human endometrium: expression, regulation, and function throughout the menstrual cycle and in early pregnancy. J Clin Endocrinol Metab 2003; 88:3885–3892.